

In situ Na·Cu₃(BTC)₂ and Li·Cu₃(BTC)₂ nanoporous MOFs synthesis for enhancing H₂ storage at ambient temperature

Mansoor Anbia¹ · Mojtaba Faryadras¹

Received: 9 May 2015 / Accepted: 1 July 2015 / Published online: 15 July 2015
© The Author(s) 2015. This article is published with open access at Springerlink.com

Abstract Na·Cu₃(BTC)₂ and Li·Cu₃(BTC)₂ (MOF) were synthesized using in situ sodium and lithium doping as hydrogen adsorbing materials. Phase stability and microstructure of the Na·Cu₃(BTC)₂ and Li·Cu₃(BTC)₂ materials were characterized by FT-IR, XRD, SEM, BET, and TGA. After in situ ions doping, the basic structures of Na·Cu₃(BTC)₂ and Li·Cu₃(BTC)₂ materials were not changed, but the surface area increased from 1300 to 1434 and 1445 m² g⁻¹, and the amount of hydrogen adsorbed increased from 1 to 1.4 and 1.6 wt% for Na·Cu₃(BTC)₂ and Li·Cu₃(BTC)₂ materials, respectively. Enhancement of hydrogen adsorption after sodium and lithium ion doping could be due to physical interaction (binding energy interaction) between hydrogen molecules and sodium ions and also due to increase of the surface area. It maybe that sodium and lithium ions act as an additional adsorption sites and adsorb hydrogen molecules.

Keywords Hydrogen adsorption · Metal–organic framework · (Cu₃(BTC)₂) · Sodium doping · Lithium doping

Introduction

Energy is an essential requirement for the development of the modern society. Therefore, energy is a key consideration in discussions of sustainable development. Renewable

resources, such as solar energy, winds, waves, and tides are environmental friendly [1]. Hydrogen gas is the ideal energy carrier, due to its zero pollution and high energy density, which is nearly three times that of gasoline [2]. In April 2009, the DOE set the new targets for on-board hydrogen storage systems: 0.045 kg kg⁻¹ for system gravimetric capacity and 0.028 kg L⁻¹ for system volumetric capacity by the year 2010, and 0.055 kg kg⁻¹ and 0.040 kg L⁻¹ by 2011 [3] at an operating temperature of 233–333 K under a maximum delivery pressure of 100 bar [2]. Main challenge in developing this technology is hydrogen storage [4].

Two different storage technologies are conventionally used, i.e. hydrogen gas in high-pressure tanks made of steel or composite material, and liquid hydrogen in cryogenic vessels [5]. Scientists are looking for novel candidate materials which can hold sufficient hydrogen in terms of gravimetric and volumetric densities [3]. An optimum hydrogen storage material must have the following characteristics: (1) high volumetric/gravimetric hydrogen storage capacity, (2) fast absorption kinetics, (3) near room temperature and ambient pressure operation, (4) light weight materials, and (5) low-cost materials [6]. The promising methods include chemical and physical storage. The emergence of many relevant reviews reflects that the field of hydrogen storage materials is receiving much attention [5].

However, so far none is capable of satisfying all the requirements of DOE criteria of size, recharging, kinetics, cost, and safety required for use in transportation [7]. So, a great challenge is the design of new porous materials possessing strong adsorption sites which enable the storage of large amounts of H₂ at low pressures [8]. Yaghi and co-workers first reported the hydrogen adsorption properties of MOF-5 at both 78 K and ambient temperature [9]. Metal–

✉ Mansoor Anbia
anbia@iust.ac.ir

¹ Research Laboratory of Nanoporous Materials, Faculty of Chemistry, Iran University of Science and Technology, Farjam Street, Narmak, 16846-13114 Tehran, Iran

organic frameworks (MOFs) are crystalline solids that are assembled by the connection of metal ions or clusters through molecular bridges [10]. MOFs have the highest specific surface areas for porous materials (up to $6200 \text{ m}^2 \text{ g}^{-1}$) and large internal pore volumes with well-defined pore size and apertures [11]. Another interesting feature of MOFs is the great variety of cations, which can participate in the framework [12]. MOFs have attracted worldwide attention in the area of hydrogen energy, particularly for hydrogen storage [3]. These materials store hydrogen in molecular form at low temperatures. Within the micropores the hydrogen is effectively compressed to a high density, resulting in an increase in the volumetric density of the hydrogen in comparison to free gas at the same temperature and pressure [13]. Although some MOFs exhibit remarkable hydrogen storage capacity with maximum hydrogen uptake up to 11 wt%, which exceeds the 2010 DOE hydrogen storage target of 6.0 wt%, and the required low adsorption temperature impedes onboard storage applications. The low uptake temperature is mainly ascribed to the low hydrogen binding energy between the guest H_2 molecule and the MOF host framework, which governs adsorption in materials ranging from microporous solids to metal hydrides [14]. $\text{Cu}_3(\text{BTC})_2(\text{H}_2\text{O})_3$, the so-called Cu-BTC, consists of dimeric Cu(II) paddlewheel units with copper dimers as four connectors and benzene-1,3,5-tricarboxylate as three connectors, forming a cubic, wide-open framework [15]. BasoliteTM C300 [16] has unsaturated Cu^{2+} sites and abundant micropores, e.g. 3.5, 5.0, and 9.0 Å small pores [17]. The shortening of the Cu–Cu distance and the distortion of the Cu–O bonds causes the appearance of coordinatively unsaturated Cu^{2+} ion sites. The large (hydrophilic) square-shaped pores, of about 0.9 nm diameter, are formed by 12 $\text{Cu}_2(\text{COO})_4$ paddlewheel subunits, forming a cuboctahedron. A second pore system of tetrahedron-shaped side pockets, of about 0.5 nm diameter, is built up from four benzene rings that constitute the inner surface with the centers of the rings forming a tetrahedron. These additional pockets are accessible from the larger pores through triangular windows of ca. 0.35 nm diameter [18]. Hydrogen molecules gradually fill the pores from 3.5 to 9.0 Å because the smaller pores have the stronger affinity towards hydrogen due to the overlap of potential fields of two opposing walls. Furthermore, the presence of a number of open metal sites in the $\text{Cu}_3(\text{BTC})_2$ enhanced its adsorption ability. Therefore, the small pore size and open metal sites in the $\text{Cu}_3(\text{BTC})_2$ material improve significantly the H_2 adsorption capacity at low pressure and at 77 K [17]. The enthalpy of adsorption reflects the binding energy between a guest molecule and its host framework. If porous MOFs can bind hydrogen molecules via interactions stronger than Van der Waals forces but weaker than molecular hydrogen bonds, they

offer a possible hydrogen storage option with improved temperature characteristics [14]. To enhance hydrogen binding energy on MOF frameworks, an important report on modified MOFs has changed the status of hydrogen storage in porous MOFs [14]. Various approaches have been pursued for improving the hydrogen adsorption characteristics in these materials [19]. Metal site exposure, metal doping, impregnation, hydrogen spillover, and cationation are currently being investigated [20]. Alkali metal atoms have been found to be good candidates for decorating the MOF structure, because of their low cohesive energies, which can avoid the clustering problem. Much of the recent work has thus been focused on Li-doped MOFs and COFs for hydrogen storage [19]. In this study, $\text{Na-Cu}_3(\text{BTC})_2$ and $\text{Li-Cu}_3(\text{BTC})_2$ materials were synthesized using in situ sodium and lithium doping and then the amount of hydrogen adsorbed was measured. So far, some studies report hydrogen adsorption in MMOFs at cryogenic temperatures. Very few ambient temperature hydrogen storage data on MMOFs are available [21]. Since the onboard storage of hydrogen at room temperature is most relevant for practical applications, we have systematically investigated hydrogen adsorption on $\text{Li-Cu}_3(\text{BTC})_2$ and $\text{Na-Cu}_3(\text{BTC})_2$ materials at ambient temperature and elevated pressures.

Experimental

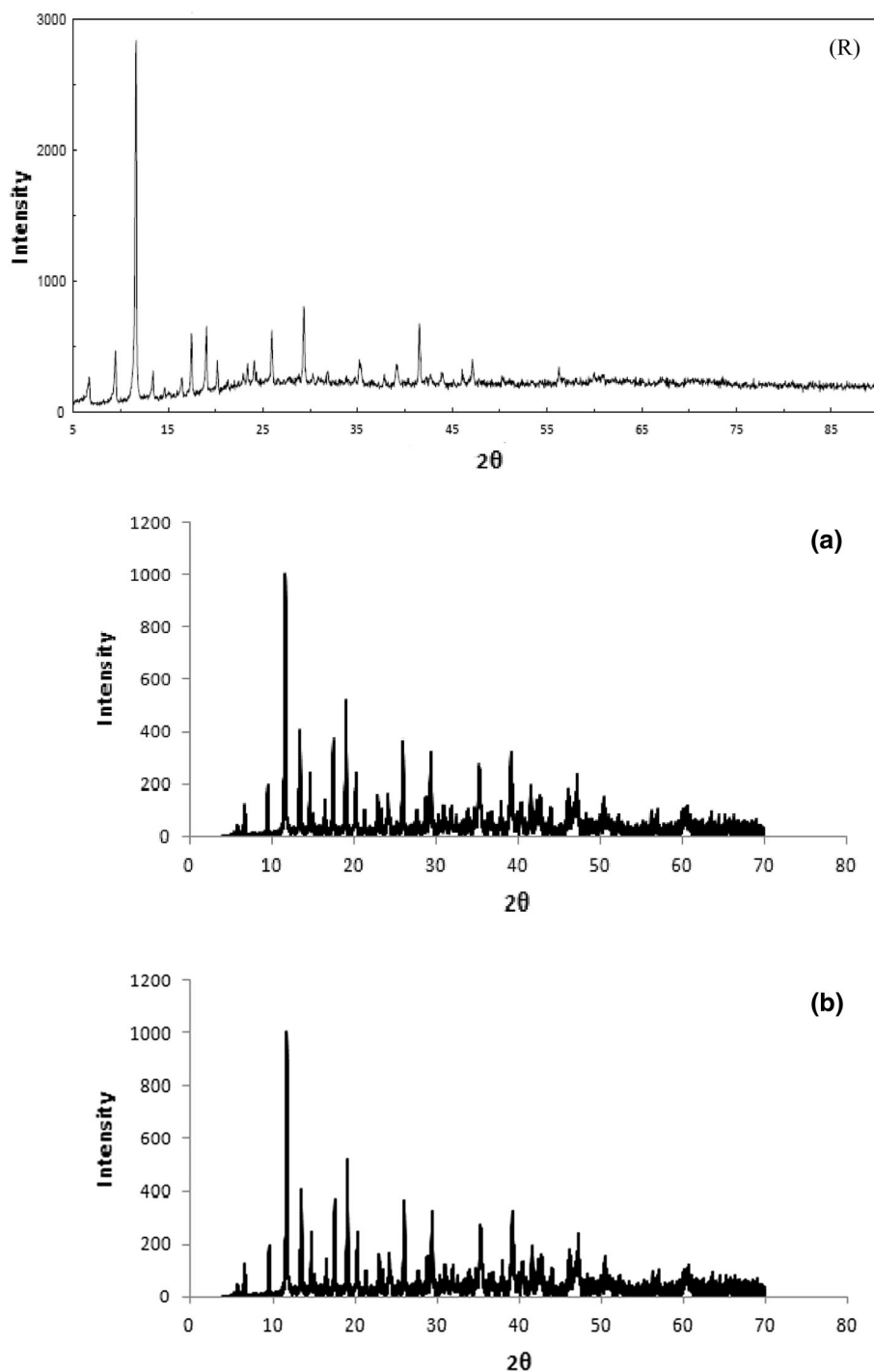
Materials

Cupric nitrate trihydrate ($\text{Cu}(\text{NO}_3)_2 \cdot 3\text{H}_2\text{O}$, 99.5 %), trimesic acid (benzene-1,3,5-tricarboxylic acid (H_3BTC , 95 %), sodium acetate trihydrate ($\text{CH}_3\text{COONa} \cdot 3\text{H}_2\text{O}$, 98 %), lithium acetate ($\text{C}_2\text{H}_3\text{LiO}_2 \cdot 2\text{H}_2\text{O}$, 98 %), and ethanol (96 %) were from E. Merck. Deionized water was used for the preparation of aqueous solutions and washing purposes.

In situ synthesis of $\text{Na-Cu}_3(\text{BTC})_2$ and $\text{Li-Cu}_3(\text{BTC})_2$ MOF materials

$\text{Na-Cu}_3(\text{BTC})_2$ and $\text{Li-Cu}_3(\text{BTC})_2$ materials were prepared using a hydrothermal method reported earlier [22]. The cupric nitrate trihydrate 2.327 g (9.6 mmol) was dissolved into 24 mL deionized water. It was followed by the addition of trimesic acid (benzene-1,3,5-tricarboxylic acid, 1.414 g (6.7 mmol)) to 24 mL of solvent consisting of equal parts of ethanol and deionized water and mixed thoroughly until it was completely dissolved. Sodium acetate, 0.5317 g (3.9 mmol), was added in situ during the synthesis of $\text{Cu}_3(\text{BTC})_2$ along with the raw materials to synthesize $\text{Li-Cu}_3(\text{BTC})_2$ and $\text{Na-Cu}_3(\text{BTC})_2$ MOF. The

Fig. 1 X-ray diffraction patterns of (R) reference: $\text{Cu}_3(\text{BTC})_2$, **a** $\text{Li}\cdot\text{Cu}_3(\text{BTC})_2$ and **b** $\text{Na}\cdot\text{Cu}_3(\text{BTC})_2$



resultant solution mixture was transferred into a 250-mL Teflon-lined stainless steel autoclave. It was kept at 393 K for 15 h in oven to yield small crystals. Then the autoclave was cooled down to room temperature, and the blue crystals were isolated by filtration. The materials were washed with the mixture of deionized water and ethanol (10:20) several times and then dried at 150 °C. The phase stability and microstructure of the $\text{Na}\cdot\text{Cu}_3(\text{BTC})_2$ and

$\text{Li}\cdot\text{Cu}_3(\text{BTC})_2$ were characterized in terms of their properties and structures, using a number of analytical techniques including X-ray diffraction (XRD; BRUKER D8A, Germany, $\text{Cu}\text{-K}\alpha$ radiation, $20\text{--}70^\circ$) and scanning electron microscopy (SEM; Hitachi model SEM3500, Japan) equipped with energy dispersive spectroscopy (EDS). The porosities and specific surface areas were measured with a Micromeritics ASAP 2020 using nitrogen

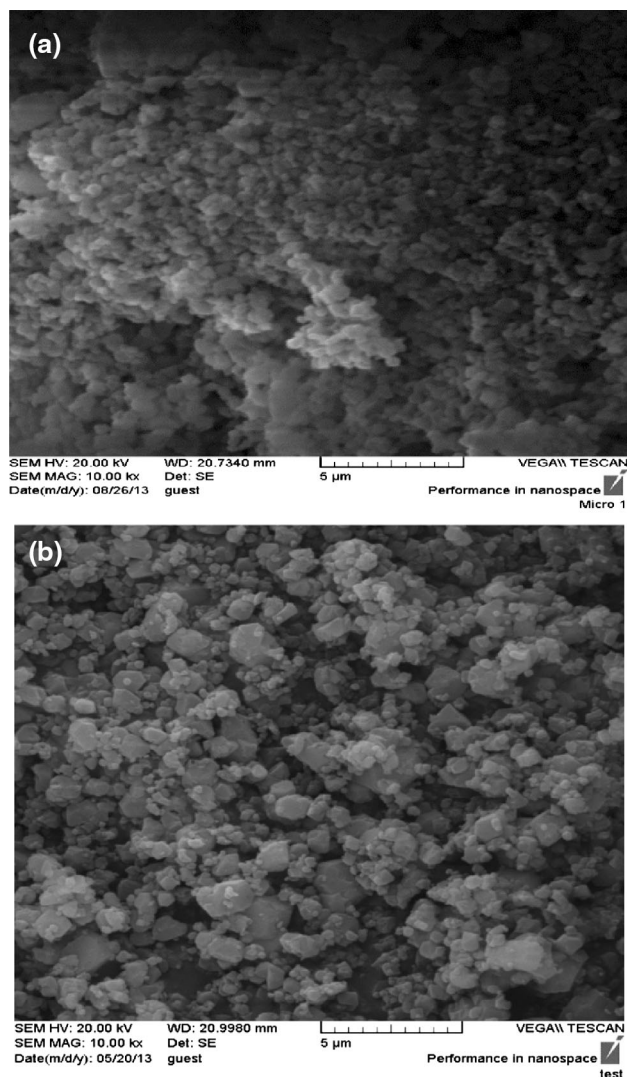


Fig. 2 Surface morphology of **a** $\text{Li}\cdot\text{Cu}_3(\text{BTC})_2$ and **b** $\text{Na}\cdot\text{Cu}_3(\text{BTC})_2$

gas at 77 K. Before the measurements, the samples were heated at 120 °C under vacuum for 1.5 h. The hydrogen adsorption measurement (volumetric method) was measured at 298 K and 15 bar pressure using the same gas sorption apparatus. Before the hydrogen-uptake measurement, the samples were heated at 120 °C in vacuum for 1.5 h.

Results and discussion

The phase stability was examined with XRD method. Figure 1 shows XRD patterns of $(\text{Li}\cdot\text{Cu}_3(\text{BTC})_2)$ and $\text{Na}\cdot\text{Cu}_3(\text{BTC})_2$ MOF materials. The main peaks and the corresponding crystal planes are identified. The main peaks of the $\text{Li}\cdot\text{Cu}_3(\text{BTC})_2$ and $\text{Na}\cdot\text{Cu}_3(\text{BTC})_2$ materials appeared at $2\theta = 11.6^\circ$ corresponding to $d = 7.6^\circ$. It

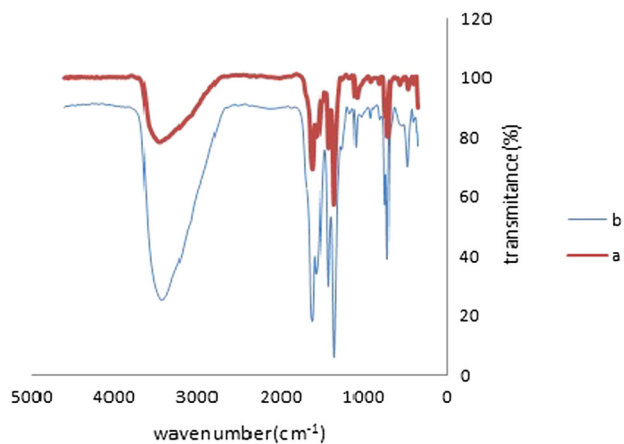


Fig. 3 IR spectra of **a** $\text{Li}\cdot\text{Cu}_3(\text{BTC})_2$ and **b** $\text{Na}\cdot\text{Cu}_3(\text{BTC})_2$

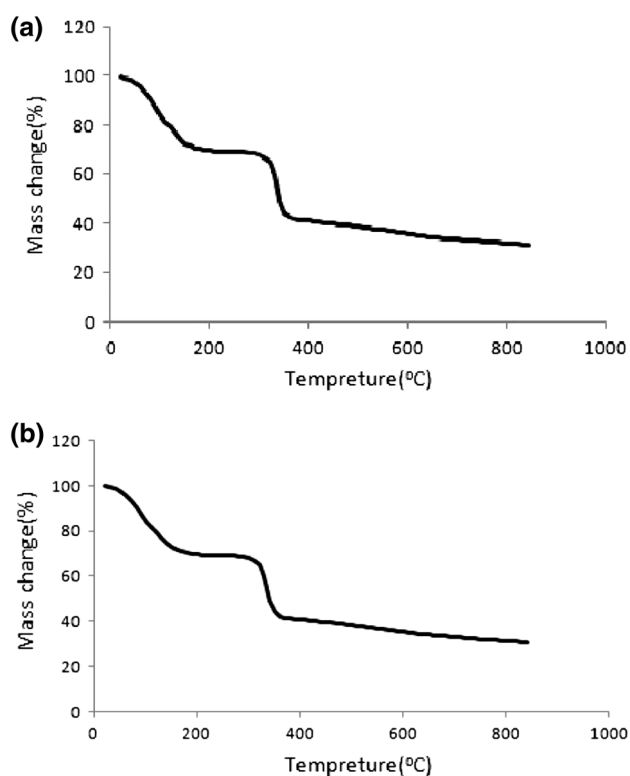
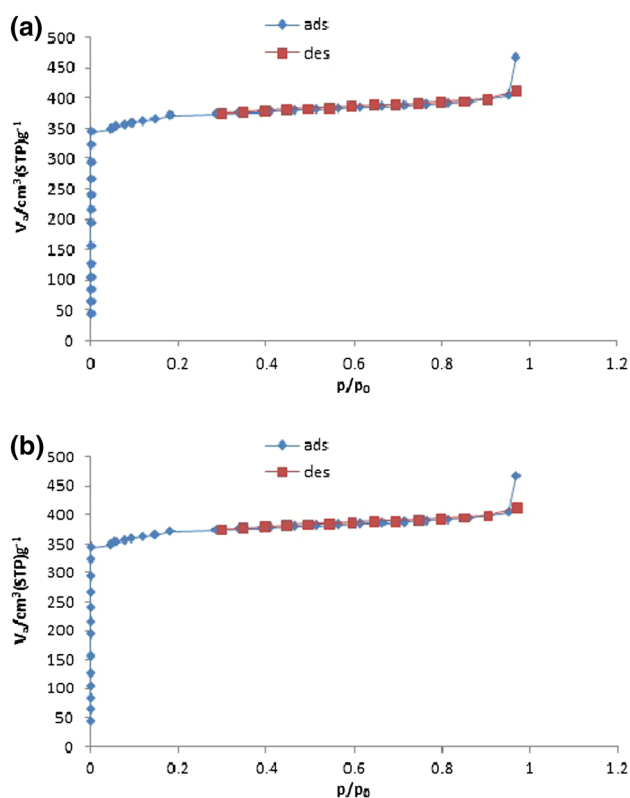
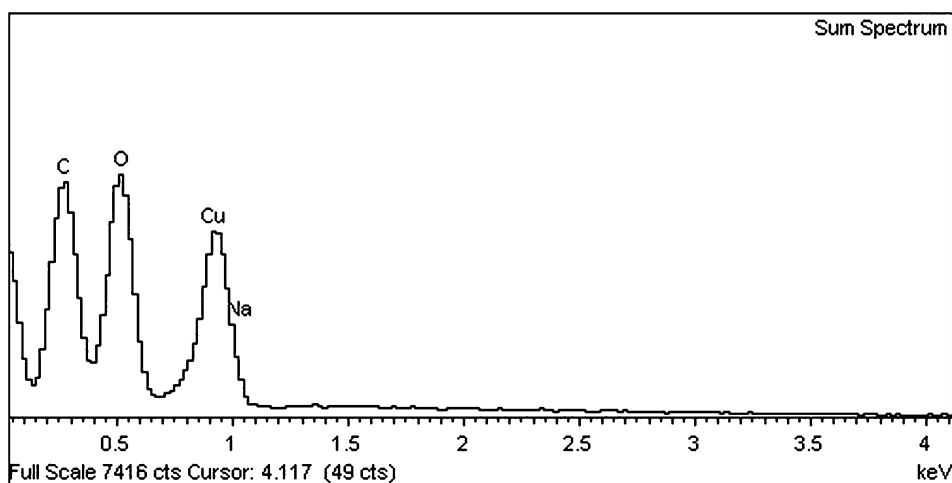


Fig. 4 TGA plots of **a** $\text{Li}\cdot\text{Cu}_3(\text{BTC})_2$ and **b** $\text{Na}\cdot\text{Cu}_3(\text{BTC})_2$

should be noted that the positions of the XRD peaks of $\text{Cu}_3(\text{BTC})_2$ doped with moderate quantities of Li, Na ($\text{Li}\cdot\text{Cu}_3(\text{BTC})_2$, and $\text{Na}\cdot\text{Cu}_3(\text{BTC})_2$) are similar to those of undoped $\text{Cu}_3(\text{BTC})_2$ [23]. It can be inferred that both undoped $\text{Li}\cdot\text{Cu}_3(\text{BTC})_2$ and $\text{Cu}_3(\text{BTC})_2$ doped with moderate quantities of Li and Na have the same main cubic structures.

The SEM images of the $\text{Li}\cdot\text{Cu}_3(\text{BTC})_2$ and $\text{Na}\cdot\text{Cu}_3(\text{BTC})_2$ samples are shown in Fig. 2. Dimensions of samples particles are approximately 2 μm . Variations in the

Fig. 5 EDAX spectrum of $\text{Na}\cdot\text{Cu}_3(\text{BTC})_2$ **Fig. 6** Comparison of N_2 adsorption (blue symbols) and desorption (red symbols) isotherms at 77 K of **a** $\text{Li}\cdot\text{Cu}_3(\text{BTC})_2$ and **b** $\text{Na}\cdot\text{Cu}_3(\text{BTC})_2$

crystal structure of the $\text{Li}\cdot\text{Cu}_3(\text{BTC})_2$ and $\text{Na}\cdot\text{Cu}_3(\text{BTC})_2$ samples are the main reason for the differences in their porous and textural properties.

The FT-IR spectra ($4600\text{--}360\text{ cm}^{-1}$) were obtained with a resolution of 4 cm^{-1} at room temperature with a Shimadzu model of 8400S spectrometer, fitted with a DLATGS detector. The samples were previously prepared as KBr mixtures. Figure 3 shows the spectra of

$\text{Li}\cdot\text{Cu}_3(\text{BTC})_2$ and $\text{Na}\cdot\text{Cu}_3(\text{BTC})_2$ samples. According to presence possibility of MOFs, sharp and strong bands in the range of $1400\text{--}1600\text{ cm}^{-1}$ refer to stretching vibrations band related to C=C bond in the aromatic ring. The presence of a weak band at 3070 cm^{-1} related to C–H is an evidence for the presence of aromatic ring. The presence of aromatic ring indicates that organic ligand used in the final sorbent structure has remained as such and not destroyed. The band around $1560\text{--}1650\text{ cm}^{-1}$ can be assigned to vibration of C=O group and the broad bands around $2400\text{--}3400\text{ cm}^{-1}$ can be associated with OH of water and ethanol. The FT-IR spectra in this figure are similar to those of the previous reports [24] and no certain change in the position and shape of the bands have been found, which indicates that the structure of the compound is preserved.

The thermal behavior of $\text{Li}\cdot\text{Cu}_3(\text{BTC})_2$ and $\text{Na}\cdot\text{Cu}_3(\text{BTC})_2$ samples (Fig. 4), shows that the initial weight loss up to $100\text{ }^\circ\text{C}$ is due to the loss of water and other guest molecules from the framework. The molecular formula of $\text{Li}\cdot\text{Cu}_3(\text{BTC})_2$ and $\text{Na}\cdot\text{Cu}_3(\text{BTC})_2$ samples is assumed as $\text{Li}\cdot\text{Cu}_3(\text{BTC})_2(\text{H}_2\text{O})_3\cdot x\text{H}_2\text{O}$ and $\text{Li}\cdot\text{Cu}_3(\text{BTC})_2(\text{H}_2\text{O})_3\cdot x\text{H}_2\text{O}$, respectively, and number of crystal water (x) about 3.0. After that, the sample does not show any significant weight change up to $320\text{ }^\circ\text{C}$ and then gradually starts losing weight. This result confirms the stability of the framework at higher temperature and there are almost no impurities on the structure. A sudden weight change (around 30.08 wt%) is observed at $321\text{ }^\circ\text{C}$ due to the total damage of BTC linker and the remaining product was CuO. This high thermal stability of $\text{Li}\cdot\text{Cu}_3(\text{BTC})_2$ and $\text{Na}\cdot\text{Cu}_3(\text{BTC})_2$ samples is favorable for use then in various applications, such as hydrogen gas storage unit integrated to a fuel cell processor.

EDAX spectrum of $\text{Na}\cdot\text{Cu}_3(\text{BTC})_2$ sample is shown in Fig. 5. It is observed that the content of Cu and Na is about 0.26 and 30.94 % in $\text{Na}\cdot\text{Cu}_3(\text{BTC})_2$ sample.



Table 1 Textural properties of $\text{Cu}_3(\text{BTC})_2$, $\text{Li}\cdot\text{Cu}_3(\text{BTC})_2$, and $\text{Na}\cdot\text{Cu}_3(\text{BTC})_2$

Material	BET surface area ($\text{m}^2 \text{g}^{-1}$)	BJH pore volume ($\text{cm}^3 \text{g}^{-1}$)	Mean pore diameter (nm)
$\text{Cu}_3(\text{BTC})_2$	1370	0.05	1.67
$\text{Na}\cdot\text{Cu}_3(\text{BTC})_2$	1433	0.18	1.10
$\text{Li}\cdot\text{Cu}_3(\text{BTC})_2$	1445	0.74	2.04

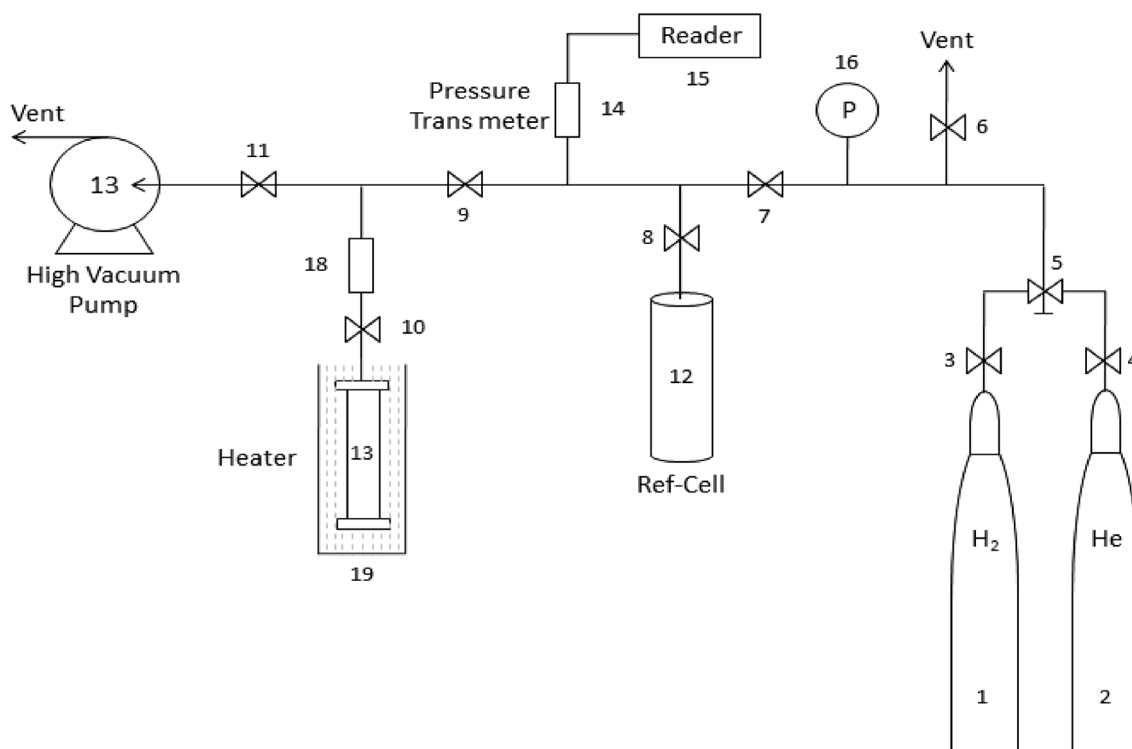
The pore size distribution, number of pores, and exposed surface area have been calculated using the results of N_2 adsorption measurements performed on an ASAP 2020 analyzer with built-in software. The N_2 adsorption/desorption isotherms of $\text{Li}\cdot\text{Cu}_3(\text{BTC})_2$ and $\text{Na}\cdot\text{Cu}_3(\text{BTC})_2$ samples at 77 K are shown in a type I curve (Fig. 6) [22]. The surface area of $\text{Cu}_3(\text{BTC})_2$ doped with Li and Na increases from 1300 to 1434 and 1445 $\text{m}^2 \text{g}^{-1}$ for $\text{Li}\cdot\text{Cu}_3(\text{BTC})_2$ and $\text{Na}\cdot\text{Cu}_3(\text{BTC})_2$ samples, respectively (Table 1).

Hydrogen adsorption measurement

A homemade setup (Fig. 7) was used for the $\text{Li}\cdot\text{Cu}_3(\text{BTC})_2$ and $\text{Na}\cdot\text{Cu}_3(\text{BTC})_2$ samples' hydrogen storage capacity measurement. The volumetric method for hydrogen uptake measurement is extensively adopted because of its simplicity, low cost, and easy assemblage [25]. At first, 1 g of

a sample was loaded in the adsorption reactor (13) and attached to the system. Then, the existing gas inside the system was swept out with helium. To degas the system, the valves 8, 9, 11, and 18 were opened and other valves closed. Then the vacuum pump was turned on, and the system was vacuumed along with the heating temperature of 473 K for 1.5 h (without any loss of crystallinity under the given thermal conditions). After degassing, the system was cooled to ambient temperature. The hydrogen was adsorbed by opening the valves 3, 4, 5, 7, 8, 9, and 10, and closing all other valves. The pressure of HP vessel decreased due to some dead volume in the reactor (including hollow space and the connected tubes) and some adsorption. By measuring the dead volumes, the exact pressure decrease due to hydrogen adsorption is calculated.

The isotherms of hydrogen adsorption on $\text{Cu}_3(\text{BTC})_2$, $\text{Na}\cdot\text{Cu}_3(\text{BTC})_2$, and $\text{Li}\cdot\text{Cu}_3(\text{BTC})_2$ samples are presented in Fig. 8. The data obtained for $\text{Cu}_3(\text{BTC})_2$ doped with alkali metal cations (Li and Na) are compared with those obtained for unmodified $\text{Cu}_3(\text{BTC})_2$. It is interesting to note that the H_2 storage capacity of $\text{Cu}_3(\text{BTC})_2$ doped with Lithium ions is higher than that of $\text{Cu}_3(\text{BTC})_2$ and $\text{Na}\cdot\text{Cu}_3(\text{BTC})_2$ samples. The remarkable decrease in the surface area at high doping levels suggest that the dopant itself (Li and Na) may ultimately block pores and prevent access to some portions of the MOF, particularly if the dopant ions present with solvent molecules; therefore, in

**Fig. 7** Setup for sorption/desorption capacity test

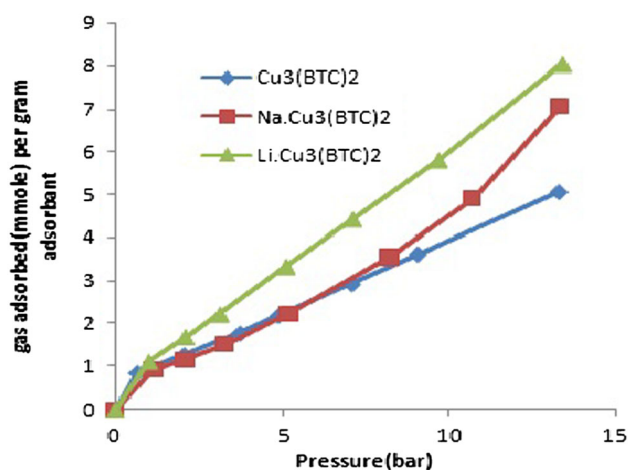


Fig. 8 Hydrogen adsorption isotherms of $\text{Cu}_3(\text{BTC})_2$, $\text{Li-Cu}_3(\text{BTC})_2$ and $\text{Na-Cu}_3(\text{BTC})_2$

this study moderate amount of dopants were used. In addition, the argument against the dominant role of dopants as special sorption sites is based on the results of experiments in which the level of doping was varied. It is clear that the adsorption of hydrogen in MOF materials depends on the specific surface area and the density of pores within the adsorbent.

Conclusions

MOF are porous hydrogen adsorbents with unusually high surface area. In this study $\text{Cu}_3(\text{BTC})_2$ (doped and undoped) MOFs were synthesized from readily available and cheap raw materials using a simple procedure. The results have shown that doping Li and Na alkali metals in the MOF structure does not change the main structure of the MOF, but causes an obvious increase in hydrogen adsorption performance of $\text{Cu}_3(\text{BTC})_2$ at ambient conditions, and this improvement may be due to Van der Waals and charge-quadrupole interactions with hydrogen gas molecules. Due to low cost, simplicity, and high adsorption performance of the proposed adsorbent, it can be a good candidate for hydrogen storage at room temperature.

Open Access This article is distributed under the terms of the Creative Commons Attribution 4.0 International License (<http://creativecommons.org/licenses/by/4.0/>), which permits unrestricted use, distribution, and reproduction in any medium, provided you give appropriate credit to the original author(s) and the source, provide a link to the Creative Commons license, and indicate if changes were made.

References

- Dutta, S.: A review on production, storage of hydrogen and its utilization as an energy resource. *J. Ind. Eng. Chem.* **20**, 1148–1156 (2014)
- Xiang, Z., Cao, D.: Porous covalent–organic materials: synthesis, clean energy application and design. *J. Mater. Chem. A* **1**, 2691–2718 (2013)
- Sculley, J., Yuan, D., Zhou, H.: The current status of hydrogen storage in metal–organic frameworks—updated. *Energy Environ. Sci.* **4**, 2721–2735 (2011)
- Anbia, M., Hoseini, V., Sheykhi, S.: Sorption of methane, hydrogen and carbon dioxide on metal–organic framework, iron terephthalate (MOF-235). *J. Ind. Eng. Chem.* **18**, 1149–1152 (2012)
- Stergiannakos, T., Tylianakis, E., Klontzas, E., Trikalitis, P.N., Froudakis, G.E.: Hydrogen storage in novel Li-doped corrole metal–organic frameworks. *J. Phys. Chem. C* **116**, 8359–8363 (2012)
- Balat, M.: Potential importance of hydrogen as a future solution to environmental and transportation problems. *Int. J. Hydrog. Energy* **33**, 4013–4029 (2008)
- Li, Y., Yang, R.T.: Hydrogen storage in metal–organic and covalent–organic frameworks by spillover. *AIChE J.* **54**(1), 269–279 (2008)
- Panella, B., Hönes, K., Müller, U., Trukhan, N., Schubert, M., Pütter, H., Hirscher, M.: Desorption studies of hydrogen in metal–organic frameworks. *Angew. Chem. Int. Ed.* **47**, 2138–2142 (2008)
- Hu, X., Fan, M., Towler, B.F., Radosz, M., Bell, D.A., Plumb, O.A.: Hydrogen adsorption and storage. In: Andrew, W. (ed.) *Coal Gasification and its Applications*, pp. 157–245. Elsevier, London (2010)
- Rowell, J.L.C., Yaghi, O.M.: Strategies for hydrogen storage in metal–organic frameworks. *Angew. Chem. Int. Ed.* **44**, 4670–4679 (2005)
- Morozan, A., Jaouen, F.: Metal organic frameworks for electrochemical applications. *Energy Environ. Sci.* **5**, 9269–9290 (2012)
- Férey, G.: Hybrid porous solids: past, present, future. *Chem. Soc. Rev.* **37**, 191–214 (2008)
- Broom, D.: *Hydrogen Storage Materials: The Characterisation of Their Storage Properties*. Springer, London (2011)
- Zou, R., Abdel-Fattah, A.I., Xu, H., Zhao, Y., Hickmott, D.D.: Storage and separation applications of nanoporous metal–organic frameworks. *CrystEngComm* **12**, 1337–1353 (2010)
- Panella, B., Hirscher, M., Pütter, H., Müller, U.: Hydrogen adsorption in metal–organic frameworks: Cu–MOFs and Zn–MOFs compared. *Adv. Funct. Mater.* **16**, 520–524 (2006)
- Moellmer, J., Moeller, A., Dreisbach, F., Glaeser, R., Staudt, R.: High pressure adsorption of hydrogen, nitrogen, carbon dioxide and methane on the metal–organic framework HKUST-1. *Microporous Mesoporous Mater.* **138**, 140–148 (2011)
- Gao, S., Zhao, N., Shu, M., Che, S.: Palladium nanoparticles supported on MOF-5: a highly active catalyst for a ligand- and copper-free Sonogashira coupling reaction. *Appl. Catal. A* **388**, 196–201 (2010)
- Krkljus, I., Hirscher, M.: Characterization of hydrogen/deuterium adsorption sites in nanoporous Cu–BTC by low-temperature thermal-desorption mass spectroscopy. *Microporous Mesoporous Mater.* **142**, 725–729 (2011)
- Srinivasu, K., Ghosh, S.K.: Tuning the metal binding energy and hydrogen storage in alkali metal decorated MOF-5 through boron doping: a theoretical investigation. *J. Phys. Chem. C* **115**, 16984–16991 (2011)
- Reardon, H., Hanlon, J.M., Hughes, R.W., Godula-Jopek, A., Mandal, T.K., Gregory, D.H.: Emerging concepts in solid-state hydrogen storage: the role of nanomaterials design. *Energy Environ. Sci.* **5**, 5951 (2012)
- Lee, J.Y., Wu, H., Li, J.: An investigation of structural and hydrogen adsorption properties of microporous metal organic framework (MMOF) materials. *Int. J. Hydrog. Energy* **37**, 10473–10478 (2012)



22. Schlichte, K., Kratzke, T., Kaskel, S.: Improved synthesis, thermal stability and catalytic properties of the metal-organic framework compound $\text{Cu}_3(\text{BTC})_2$. *Microporous Mesoporous Mater.* **73**, 81–88 (2004)
23. Lin, K.S., Adhikari, A.K., Ku, C.N., Chiang, C.L., Kuo, H.: Synthesis and characterization of porous HKUST-1 metal organic frameworks for hydrogen storage. *Int. J. Hydrog. Energy* **37**, 13865–13871 (2012)
24. Loera-Serna, S., Oliver-Tolentino, M.A., López-Núñez, M.L., Santana-Cruz, A., Vargas, A., Cabrera-Sierra, R., Belt, H.I., Flores, J.: Electrochemical behavior of $[\text{Cu}_3(\text{BTC})_2]$ metal-organic framework: the effect of the method of synthesis. *J. Alloys Compd.* **540**, 113–120 (2012)
25. Rashidi, A.M., Nouralishahi, A., Khodadadi, A.A., Mortazavi, Y., Karimi, A., Kashefi, K.: Modification of single wall carbon nanotubes (SWNT) for hydrogen storage. *Int. J. Hydrog. Energy* **35**, 9489–9495 (2010)

